



DETERMINATION OF SAND MINING PROSPECTIVE ZONES BASED ON SEDIMENT THICKNESS ANALYSIS USING HVSR MICROTREMOR AND GRAVITY METHODS: A CASE STUDY IN CANGKRINGAN, SLEMAN, DAERAH ISTIMEWA YOGYAKARTA

Firdos Bahar Sidik¹, Muhammad Gilang Ramadeo², Maria Diyah Ayu Wulandari³, Savira Zahrul Khumairo⁴, Ekasari Nurkholijah⁵, Farizki Budi Pangestu⁶, Safina Fitrinova⁷, Haris Muhlisin⁸

^{1,2,3,4,5,6,7,8}Universitas Pembangunan Nasional "Veteran" Yogyakarta, Indonesia

Email: baharsidik.firdos@gmail.com

ARTICLE INFO

Keywords:
HVSR,
Microtremor, Sand
Mining.

ABSTRACT

Mount Merapi is the most active type A volcano, especially on the island of Java. It produces sediment products totaling 140 million m³ located at the peak of Mount Merapi, descending through the mountain slopes to rivers originating from Mount Merapi. This sediment is subsequently utilized as a sand mining area. Therefore, it is necessary to determine prospect zones for sand mining that align with environmental, economic, and mitigation aspects in the Cangkringan area, Sleman, Yogyakarta Special Region. Seventeen microtremor measurement points were used with the Horizontal to Vertical Spectral Ratio (HVSR) method to determine sediment thickness, constituent lithology, and mining zones suitable for safety and mitigation aspects. Additionally, the gravity method was employed with 247 measurement stations obtained from GGM Plus to determine rock density and estimated thickness based on 2.5D modeling. The study resulted in the distribution of dominant soil frequencies ranging from 0.5 Hz to 7.5 Hz. High frequencies indicate old rocks, while medium frequencies suggest alluvial rocks with a thickness of ± 5 m. Low frequencies indicate alluvial rocks with a thickness exceeding ± 30 meters. Based on gravity results, the average depth is ± 90 -200 m with a density of 2.6 g/cm³, reflecting the depth of the bedrock in the study area, composed of andesitic volcanic rock. Soil vulnerability analysis in the study area classified into three categories, with values of 4.2-5.4 being highly vulnerable to surface deformation, values of 1.8-3.8 indicating moderate vulnerability, and values of -0.2-1.4 representing low vulnerability. Furthermore, the Peak Ground Acceleration (PGA) ranges from 500-1200 gal with intensity X. Ground Shaking Spectrum (GSS) data indicates that the study area experiences vibration phenomena with elastic soil dynamics. Therefore, the exploitation of sand resources in the Cangkringan area can be conducted in the southern region of Mount Merapi, approximately 2 km away from the mountain center. This is because the southern part of the research area has suitable mitigation measures. Moreover, based on the analysis, sediment thickness in this area ranges from ± 5 -30 meters.

Copyright © 2024 JSR. All rights reserved.

INTRODUCTION

Mount Merapi is the most active type A volcano, particularly on the island of Java, with eruption cycles of short intervals of 2-5 years and long intervals of 5-7 years (Rahayu et al., 2014). To date, Mount Merapi has experienced a total of 68 eruptions, with the most recent significant eruption occurring on October 26, 2010 (Harsanto, 2015; Swastiak, 2020). In that year, Mount Merapi produced sediment products totaling 140 million m³, located at the summit and descending through the mountain slopes to rivers originating from Mount Merapi (DGWR, 2010; PMVBG, 2014; Sukatja et al., 2017; Ainia, 2021).

The impact of these eruptions has led to changes in river morphology, creating new rivers filled with volcanic materials such as rocks and sand resulting from Mount Merapi's eruptions. Subsequently, these areas have been utilized for sand mining activities (Rizal, 2015; Ainia, 2021). The sand mining industry in Cangkringan, Sleman, Yogyakarta adheres to regulations based on the Regent of Sleman's Decree No. 284 of 2011 regarding the Normalization of River Flow Post-Mount Merapi Eruption (Bahtiar, 2016; Putri & Raharjo, 2018; Nender, 2018; Anjani, 2021). This adherence affects the economic sector and infrastructure, thereby motivating the local community to engage in sand mining in the Cangkringan area, Sleman, Yogyakarta Special Region.

Therefore, there is a need for exploration and determination of sand mining zones in the Cangkringan area using Gravity and Microtremor HVSR methods, taking into account environmental aspects, economic considerations, sediment thickness, and disaster mitigation.

LITERATURE REVIEW

Geomorphology

Mount Merapi is classified within geomorphic units based on the physical aspects of the constituent rocks, controlling structures, and evolving processes (Van Zuidam, 1983). Mount Merapi is analyzed as a geomorphological form of volcanic origin, which is divided into four landforms:

1. Lava Dome (IV), occupying 5% of the research area (Yudiantoro, 2023), is located at the summit of Mount Merapi. It features a hemispherical-semi-hemispherical dome morphology formed by the accumulation of thick lava in the Merapi Mountain crater. The elevation ranges from 2885 to 2900 meters above sea level (mdpl).
2. Lava Flow Slopes (V2), covering 55% of the area (Yudiantoro, 2023), exhibit steep to very steep slope morphology, with elevations ranging from 2250 to 2860 mdpl.
3. Pyroclastic Flow Slopes (V3), representing 25% of the area (Yudiantoro, 2023), are concentrated on the northwest and southwest slopes of Mount Merapi, and in the Pasarbubar Crater. The morphology consists of steep to very steep slopes, with elevations ranging from 2250 to 2750 mdpl.
4. Crater (V4), occupying 15% of the area (Yudiantoro, 2023), is concentrated at the summit of Mount Merapi, extending along the southwest slope and into the Pasarbubar Crater. The elevation ranges from 2520 to 2900 mdpl, with a slope-plateau morphology.

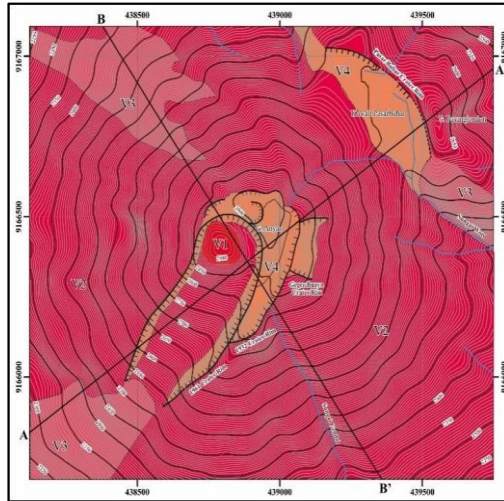


Figure 1. Volcanic Landforms (V), with the division of landforms at the summit of Mount Merapi and its surroundings (Yudiantoro, et al., 2023)

Volcanostratigraphy

Based on the volcanostratigraphy by Yudiantoro, 2023, as established by Wirakusumah et al., 1989, and Gertisser et al., 2012, the stratigraphy of Mount Merapi is divided into two main units: 'Merapi Tua' (Old Merapi) and 'Merapi Muda' (Young Merapi). These units are composed of various layers representing a sequence of ages, ranging from old to young. The stratigraphy is as follows:

1. Old Merapi, the rock unit within the Old Merapi rock unit consists solely of the Merapi 2 andesite lava flow (M12), covering 8% of the area (Yudiantoro, 2023). This unit is known as the Batulawang unit (Camus et al., 2000; Sudrajat et al., 2010) and has an age of approximately 4,300 to 4,800 years ago.
2. Young Merapi, based on Yudiantoro, 2023, the volcanostratigraphy of Young Merapi is classified into three rock/deposit units:
 - a. Merapi 3 andesite lava flow unit (M13), scattered across 3% of the entire map area, formed before the historical period of Merapi. Also includes Alep-Alep lava flows (Gertisser et al., 2012; Wirakusumah et al., 1989). Composed of andesitic igneous rocks with an age ranging from around 1,700 years ago (Wirakusumah et al., 1989).
 - b. Young pyroclastic deposits and Merapi's debris unit, covering 26% of the area, including the Brubuhan and Kaliadem pyroclastic flow deposit units (Sudrajat et al., 2010). These deposits have an age less than 1550 AD-present (Gertisser et al., 2021). They exhibit a variety of grain sizes resulting from pyroclastic flows, volcanic eruptions, and are associated with lahar and ashfall deposits from Mount Merapi (Yudiantoro, 2023).
 - c. Merapi 4 andesite lava flow deposit unit (M14), covering approximately 77% of the area. This unit is part of the Garuda lava unit, with an age less than 1883 AD-present, composed of andesitic rocks.

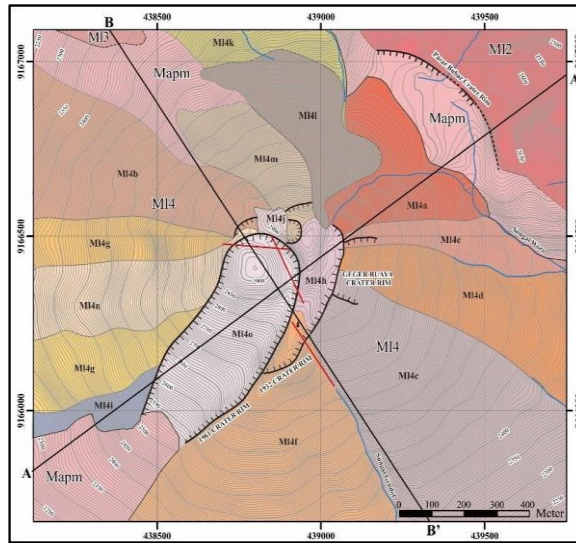


Figure 2. Geological Map of the Summit of Mount Merapi and Its Surroundings (Yudiantoro, et al., 2023).

METHOD

This research was conducted in the Cangkringan area, Sleman, Special Region of Yogyakarta, utilizing both primary measurement data in the form of Microtremor data and secondary data from the Gravity method obtained from the GGM Plus website, consisting of high-resolution Gravity data. Microtremor measurements were carried out on May 20, 2023, using a Portable Digital Short-Period Type TSD instrument. Data was collected at 17 measurement stations over approximately 40 minutes within an area of 1.3 x 1 km.

The research was specifically conducted in the Cangkringan area. Additionally, Gravity data was collected from GGM Plus, covering an area of 3 x 4 km with a total of 247 measurement stations. The processing and analysis procedures for this study are outlined in the flowchart depicted in Figure 3.

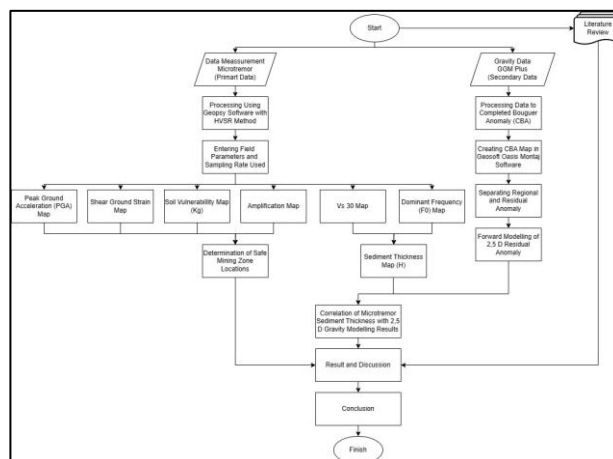


Figure 3. Flowchart

RESULTS AND DISCUSSION

Complete Bouguer Anomaly (CBA)

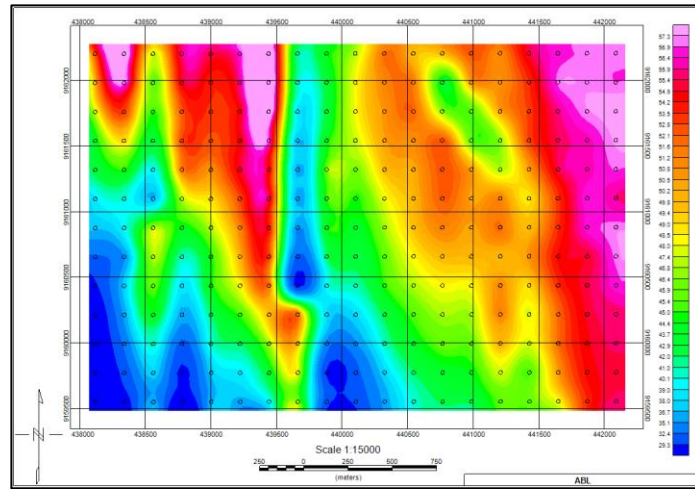


Figure 4. Map of Complete Bouguer Anomaly (CBA) Research Location

In Figure 4, a map of the Complete Bouguer Anomaly (CBA) was generated from GGM Plus data, utilizing a total of 247 measurement stations. The CBA map illustrates the combined anomaly of both regional (deep-seated) and residual (shallow) anomalies. The gravity values (mGal) distribution in the research area ranges from a maximum of 57.3 mGal to a minimum of 29.3 mGal. High gravity values in the research area are observed in the east and west directions, with the highest concentration located directly over the summit of Mount Merapi. Conversely, low gravity values dominate the southwestern part of the research area, which can be attributed to the relatively greater distance from the peak of Mount Merapi in that direction.

Separation of Regional and Residual Anomalies from CBA Map

The separation of regional and residual anomalies from the Complete Bouguer Anomaly (CBA) is intended to discern the differences in anomaly bodies. This is because the regional CBA depicts conditions beneath the deep subsurface, while the residual CBA reveals shallow anomaly bodies in the research area. The results of this anomaly separation can be observed in Figure 5, which represents the map of the Regional CBA, and Figure 6, which depicts the map of the Residual CBA.

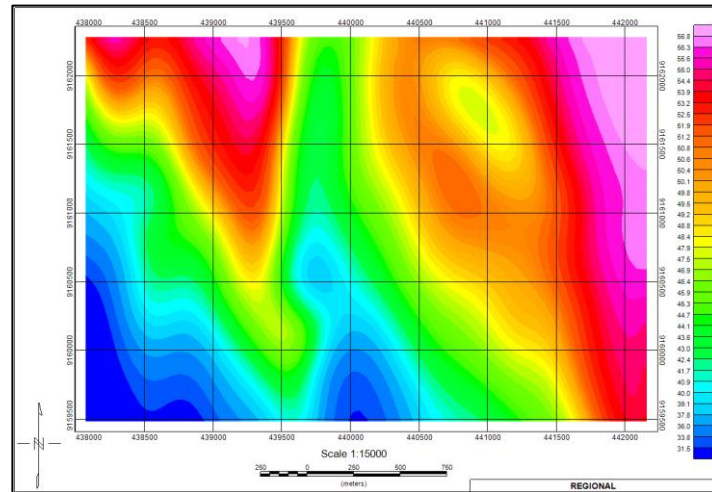


Figure 5. Regional Complete Bouguer Anomaly (CBA) Map of the Research Location

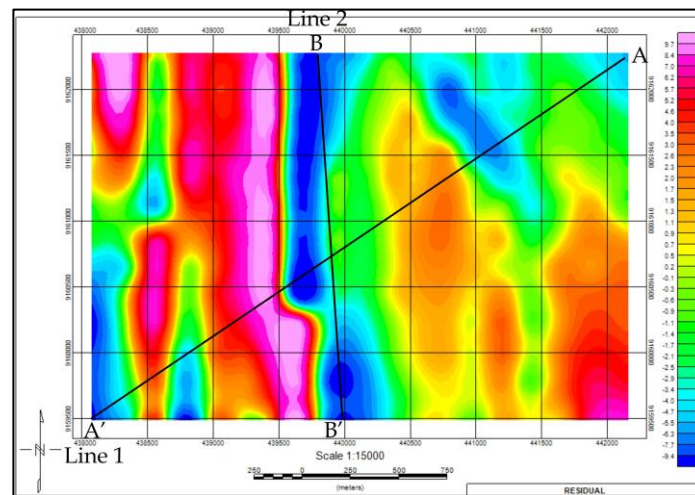


Figure 6. Residual Complete Bouguer Anomaly (CBA) Map & Cross-Section Slicing 1 and 2 at the Research Location

In Figure 5, the map of regional anomalies from the Complete Bouguer Anomaly (CBA) displays gravity values ranging from 31.5 to 56.8 mGal. The regional gravity values indicate variations in density, with higher-density values in the northeast and northwest directions, while lower-density values are observed in the southwest direction. Meanwhile, in the map of Residual CBA (Figure 6), the gravity values range from -9.4 to 9.7 mGal. The color closure in the Residual CBA map illustrates diverse variations across the entire map, reflecting the presence of shallow anomaly bodies in the research area and resulting in a more varied color closure. Low values in the Residual CBA map are concentrated in the central part, creating a continuous pattern from north to south. Additionally, high values in this research area are observed in the west direction, with continuous values from north to south.

Forward Modeling of 2.5D Residual Gravity Data

Slicing on the map of Residual Complete Bouguer Anomaly (CBA) was conducted along two profiles, namely Profile 1 and Profile 2. The purpose of these profiles was to

delineate subsurface rocks along the designated paths, which were subsequently used to create a model representing the subsurface layers. The subsurface rock model was developed using data on density, subsurface geometry, and their respective Mean Sea Level (MSL) locations, achieved through a trial-and-error process. This iterative process aimed to produce a gravity anomaly curve that best matched the observed data (Uwiduhaye et al., 2016).

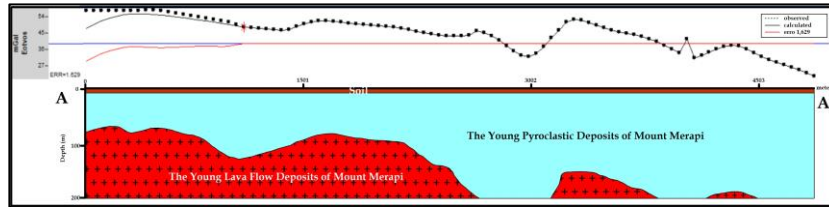


Figure 7. 2.5D Modeling Cross-Section 1 A-A' at the Research Location

Figure 6 depicts the 2.5D forward modeling along Profile 1 at the study location, oriented southwest to northeast. The local gravity in the 2.5D cross-section along Profile 1 ranges from a maximum of 55 mGal to a minimum of 27 mGal, with an estimated achieved depth of approximately 200 meters and a cut length of ± 4650 meters. In this 2.5D cross-section, the subsurface rock layers are revealed. These layers include young Merapi volcanic rocks with a density of 2.6 g/m³, young Merapi pyroclastic rocks with a density of 2.1 g/m³, and soil with a density of 1.9 g/m³. The distribution of these rocks is believed to be the result of Mount Merapi eruptions, depositing andesitic volcanic rocks that decrease in quantity as they move away from the summit due to rock solidification. The sedimentary pyroclastic rocks in the 2.5D modeling show accumulation in the northeast direction, likely resulting from previous explosive events. These sediments are expected to exhibit a variety of grain sizes, influenced by pyroclastic flow deposits (Yudiantoro, 2023).

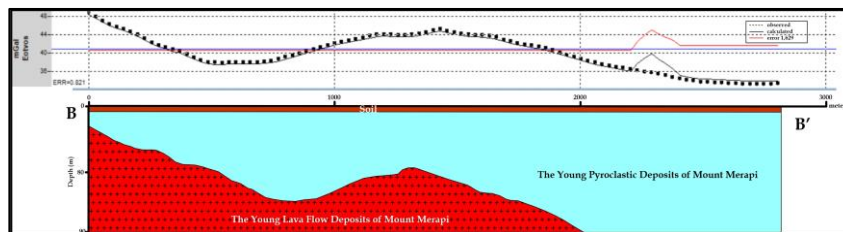


Figure 8. 2.5D Modeling Cross-Section 2 B-B' at the Research Location

Figure 7 illustrates the 2.5D forward modeling along Profile 2 at the study location, oriented north to south. The local gravity in the 2.5D cross-section along Profile 2 ranges from a maximum of 48 mGal to a minimum of 33 mGal, with an estimated achieved depth of approximately 90 meters and a cut length of ± 2800 meters. In this 2.5D cross-section, the subsurface rock layers are similar to those in Profile 1. They include young Merapi volcanic rocks with a density of 2.6 g/m³, young Merapi pyroclastic rocks with a density of 2.1 g/m³, and soil with a density of 1.9 g/m³. The distribution of these rocks is believed to be the result of Mount Merapi eruptions, depositing andesitic volcanic rocks that decrease in quantity as they move away from the summit due to rock solidification. Similarly, the sedimentary pyroclastic rocks in the 2.5D modeling show accumulation in the northeast direction, likely resulting from previous explosive events. These sediments are expected to exhibit a variety of grain sizes, influenced by pyroclastic flow deposits (Yudiantoro, 2023).

Amplification (A0)

Figure 8 represents the Amplification Map (A0), which illustrates the distribution values of amplification on seismic waves due to significant differences between layers or the amplification generated by the propagation of seismic waves in a soft medium compared to the previously traversed medium (Pancawati, 2016). A0 is essentially a value that represents the spread of values indicating the physical condition of rocks, such as their soft or hard nature, based on the propagation of seismic waves and amplification values. If the A0 value is larger, it indicates that the subsurface rocks are experiencing deformation, leading to changes in the physical properties of those rocks (Sungkono, 2011; Arifin et al., 2013)

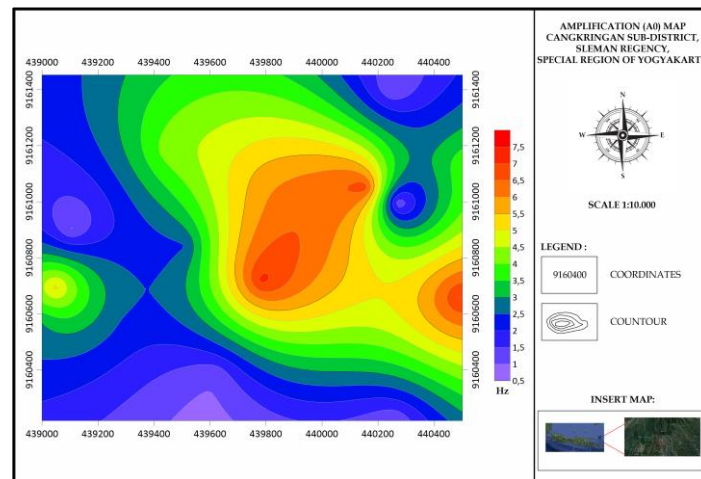


Figure 9. Amplification Map at the Research Location

Figure 8 presents the A0 values in the research area of Cangkringan, representing the hardness or softness of the underlying rocks in the study location. According to Ratdomorpuro, 2008, the classification of A0 values is divided into four categories: low, medium, high, and very high, as indicated in Table 1.

Tabel 1. Amplification Classification (Ratdomorpuro, 2008)

Zone	Classification	Amplification Values (A0)
1	Low	$A < 3$
2	Medium	$3 \leq A < 6$
3	High	$6 \leq A < 9$
4	Very High	$A \geq 9$

In Figure 8, the A0 map in the Cangkringan region is classified into three zones: low, moderate, and high, each represented by a specific color. The blue color represents the low zone, the orange-green color indicates the moderate zone, and the red color represents the high zone. On the map, low values are situated to the north and south in the research area, while the moderate zone is located between the low and high zones, centralized in the core of the research area. The amplification classification in the Cangkringan region is presented in Table 2.

Table 2. Amplification Classification at the Research Location

Zone	Classification	Amplification Values (A0)	Description
1	Low	0.5-2.5	Lithology of Hard Sedimentary Rocks
2	Medium	3-6	Lithology of Medium Sedimentary Rocks
3	High	6-7.5	Lithology of Soft Sedimentary Rocks

Dominant Frequency (f_0)

The Dominant Frequency (f_0) map depicts the distribution of values representing a frequency that arises from the properties and characteristics of the underlying rocks in a particular area. The dominant frequency value is closely related to the thickness and depth of a layer of soft sediment (Nakamura, 1989). A higher dominant frequency value indicates a thin and rigid layer.

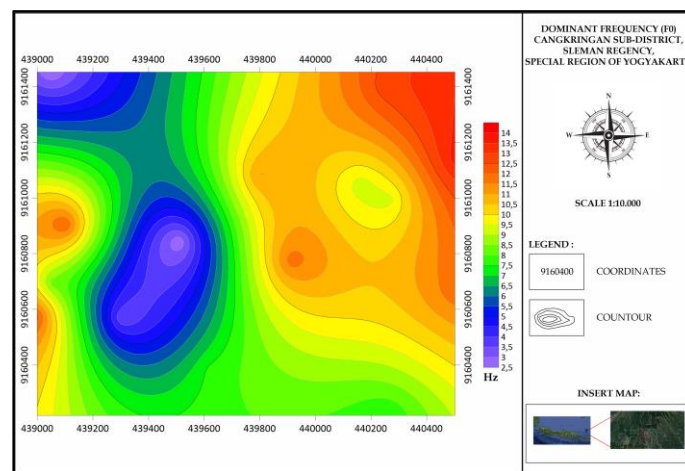


Figure 10. Map of Dominant Frequencies at the Research Location

In Figure 9, the map illustrates the values of the dominant frequency in the Cangkringan region, referring to the classification by Arifin et al., 2013, which is modified from Kanai, 1983.

Table 3. Soil Classification Table Based on Dominat Frequency Values (Arifin, dkk. 2013 Modifikasi dari Kanai, 1983).

Soil Classification	Dominant Frequency (Hz)	Kanai Classification	Description
Type I	6,67-20	Tertiary or older rock, composed of hard gravelly sandstone	Thin surface sediment layer, predominantly hard rock
Type II	10-4	Alluvial rock with a thickness of 5m. Comprising gravelly sand, hard sandy clay, clay, etc.	Surface sediment layer thickness ranging from 5 to 10m
Type III	2,5-4	Alluvial rock almost like Type II, distinguished by an unknown formation	Surface sediment layer thickness falls into the thick category, ranging from 10 to 30m
Type IV	<2,5	Alluvial rock formed from delta sedimentation,	Surface sediment layer thickness is extremely thick

topsoil, mud, soft humus soil, delta deposits, or mud deposits, soft soil with a depth of 30m

The dominant frequency in the research area is classified into four types based on the emerging frequencies. High frequencies are observed in the east and west directions of the research area, while low frequencies are located in the south, indicating deposition resulting from the eruptions of Mount Merapi that flow towards the foothills of the mountain. A detailed classification for the research area is provided in Table 4.

Table 4. Dominant Frequency Classification Table for the Study Area.

Soil Classification	Dominant Frequency (Hz)	Kanai Classification	Description
Type I	10,5-14	Tertiary or older rock, composed of hard gravelly sandstone	Thin surface sediment layer, predominantly hard rock
Type II	4,5-9,5	Alluvial rock with a thickness of 5m. Comprising gravelly sand, hard sandy clay, clay, etc.	Surface sediment layer thickness ranging from 5 to 10m
Type III	2,5-3,5	Alluvial rock almost like Type II, distinguished by an unknown formation	Surface sediment layer thickness falls into the thick category, ranging from 10 to 30m
Type IV	0,5-1,5	Alluvial rock formed from delta sedimentation, topsoil, mud, soft humus soil, delta deposits, or mud deposits, soft soil with a depth of 30m	Surface sediment layer thickness is extremely thick

Soil Vulnerability (Kg)

Soil vulnerability (Kg) is a value that describes the susceptibility of an area to earthquake risk (Saadudin et al., 2015). According to Nakamura in 2000 and 2008, soil vulnerability can determine the susceptibility of the surface to deformation during an earthquake, primarily in areas with thick sedimentary rock layers. Therefore, there is an inverse relationship between A0 and F0, which can influence the magnitude of the Kg value.

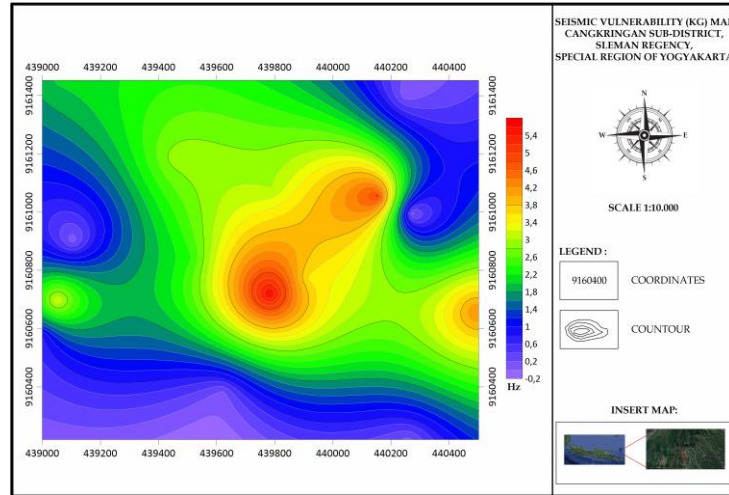


Figure 11. Seismic Vulnerability Map of the Study Area.

Referring to the classification table proposed by Daryono et al., 2009, the distribution values of Kg in the Cangkringan area in Figure 10 are classified as low values, mainly dominated by rocks originating from Mount Merapi. According to the map, high values are represented by the red-orange closure color in the central area, indicating a vulnerability range of 4.2-5.4, which is highly susceptible to surface deformation. Moderate values are represented by the green-yellow closure covering the red-orange closure, indicating moderate vulnerability with values ranging from 1.8-3.8. Meanwhile, low values are represented by the purple-blue color, ranging from -0.2 to 1.4, spreading across the entire map and covering areas with moderate to high vulnerability, indicating low soil vulnerability in that region.

From the classified soil vulnerability values, areas with high vulnerability are prone to deformation, influenced by significant amplification values but small dominant frequency values. This suggests that the region is composed of thick and soft sedimentary rocks. Moderate soil vulnerability values are interpreted as rocks with moderate amplification and dominant frequency, possibly due to deposition patterns or sedimentation close to the mountain. Meanwhile, low vulnerability values are attributed to low amplification values and high dominant frequency values, indicating that the subsurface conditions consist of hard rocks/sediments with thin thickness.

Table 5. Soil Vulnerability Classification Table (Daryono et al., 2009)

Soil Vulnerability Index	Classification
<10	Low
10 < Kg < 20	Moderate
>20	Hazardous

Peak Ground Acceleration (PGA)

The value of Peak Ground Acceleration (PGA) reflects the maximum acceleration of ground motion resulting from an earthquake. The acceleration of ground movement can be calculated based on the earthquake magnitude, distance from the previous earthquake source, and the dominant frequency that emerges at a specific location (Fatimah et al., 2018).

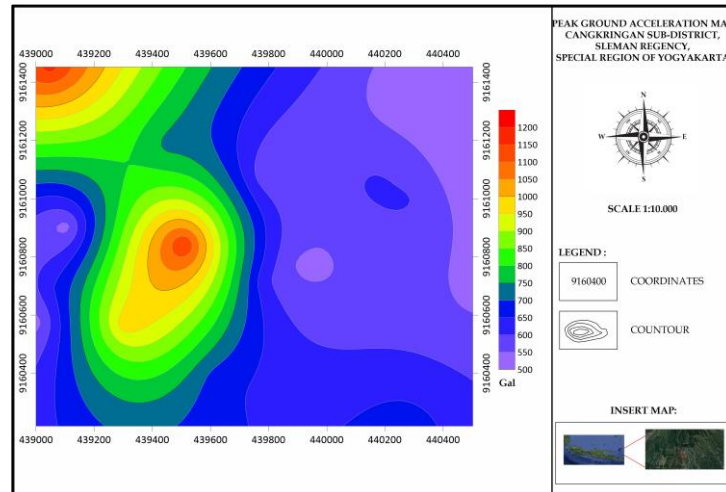


Figure 12. Map of Peak Ground Acceleration at the Research Location.

Kanai (1966) suggests that as the PGA value increases, the ground acceleration at a location generates significant energy, leading to surface damage. This classification has been detailed in Table 6.

Table 6. Scale of Earthquake Intensity Values Based on Impact and Maximum Ground Acceleration (USGS, 2016)

PGA (gal)	Intensity	Effect
1-2	I	It is not felt.
2-5	II	Felt by people at rest, especially on higher floors of buildings or elevated places.
5-10	III	Sensed inside homes, as if a truck is passing by, but many do not expect an earthquake.
	IV	Feels inside the house as if a truck is passing by or as if a heavy object is hitting the walls of the house.
10-25	V	Can be felt outside the house, causing people who are asleep to wake up, with fluids visibly moving and spilling slightly.
	VI	Felt by everyone, causing many to run outside in surprise. Pedestrians are disturbed while walking, windows are creaking, pottery and fragile items are breaking.
50-100	VII	Can be felt by drivers, causing difficulty in driving. Pedestrians find it hard to walk steadily, and weak smokestacks may break.
100-250	VIII	Driving is disrupted, and there is damage to strong buildings due to parts collapsing.
250-500	IX	The public is in panic, weak buildings collapse, strong buildings suffer severe damage with foundation and frame damage.
500-1000	X	In general, all walls, house frames, and foundations are damaged. Some strong wooden structures and bridges are damaged, severe damage occurs to dams, embankments, and fishponds, and there is a large landslide.

Based on the PGA map in Figure 11, it can be observed that the distribution values of PGA are represented by color closures, where orange-red indicates high values, green-orange indicates moderate values, and purple-blue indicates low values. According to

the classification by USGS (2016), the research area falls under intensity X with PGA values ranging from 500-1200. This suggests a very significant impact, with potential damages such as "generally, all walls, frames of houses, and foundations are damaged, some strong wooden buildings and bridges are damaged, severe damage occurs to dams, dikes, and fishponds, and large landslides occur." The high PGA values are attributed to the research area being situated on Mount Merapi, an active type A volcano that frequently experiences eruptions, leading to ground movements.

Ground Shear Strain (γ)

Ground shear strain is a value that represents the maximum deformation experienced by the surface soil (Nakamura, 1989). If the strain is high, it can lead to surface deformation and collapse. Ground shear strain is related to the dynamic properties of the soil, such that when ground shear strain is low, the resulting deformation is small, and if the value is high, the deformation will be more significant (Syahputri, 2020).

Table 7. Relationship between Ground Shear Strain (γ) Values and Soil Dynamic Properties (Ishihara, 1982)

The value of ground shear strain (γ)	$10^{-6} - 10^{-5}$	$10^{-4} - 10^{-3}$	$10^{-2} - 10^{-1}$
Phenomenon	Seismic Waves, Vibrations	Crack, Soil Settlement (Differential Settlement)	Landslide, Soil Compaction, Liquefaction
Soil Dynamics	Elastic	Elastic-Plastic	Velocity - Repetition Effect

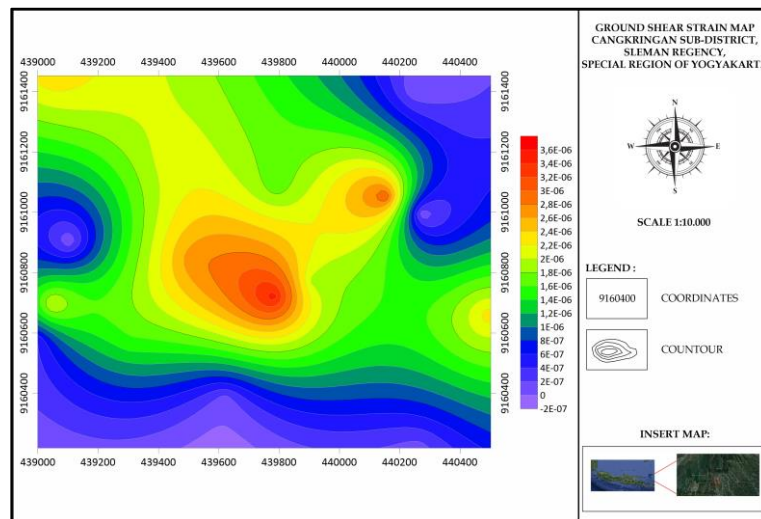


Figure 13. Map of Ground Shear Strain in the Research Area

Based on Figure 12, which is a map of ground shear strain, it forms closures represented by colors. The classification is based on the table relating ground shear strain and dynamic soil properties (Ishira, 1982). High values are located in the central area of the study with orange-red colors and values ranging from 2.4×10^{-6} to 3.6×10^{-6} . Moderate values are in green-yellow closures with values ranging from 1×10^{-6} to

2.2 x10⁻⁶. Low values are represented by purple-blue closures with values from -2 x10⁻⁷ to -8 x10⁻⁷. All three values exhibit the same phenomenon and dynamic soil properties, namely waves and vibrations with elastic characteristics.

Vs30

Vs30 represents the shear wave velocity at a depth of 30 meters, where the value of Vs30 is used to describe surface lithology (Wibowo and Huda, 2020). The Vs30 value influences the soil amplification factor. If the Vs30 value is small, then the soil amplification factor will be large. This explains that the relationship between the two is closely related to the density level of a rock (Maimun, et al., 2020).

Table 8. Soil Classification Based on Vs30 Values (UBC, 1997)

Site Classification	Vs(m/s)
Hard Rock (SA)	>1500
Rock (SB)	750-1500
Hard and Dense Soil with Rock (SC)	350-750
Moderate Soil (SD)	175-350

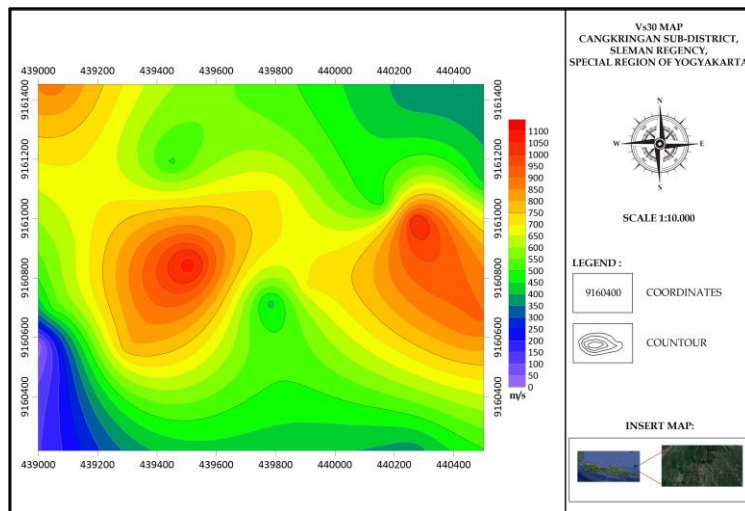


Figure 14. Vs30 Acceleration Map at the Research Location

Based on Figure 13, which is the Vs30 distribution map, it forms closures represented by colors. According to the color closures on the Vs30 distribution map above, it can be divided into three zones: high, medium, and low. The high zone is indicated by red closures with Vs30 values of 800-1100 m/s. Meanwhile, the medium zone is indicated by yellow to green closures with Vs30 values of 350->800 m/s. Finally, the low zone is indicated by blue closures with Vs30 values of 0->350 m/s.

Sediment Thickness (H)

The sediment thickness is the thickness of the weathered layer on top of the bedrock. The thickness of the sediment layer is directly proportional to the average shear wave propagation velocity and inversely proportional to the natural frequency (Satria, et al., 2020).

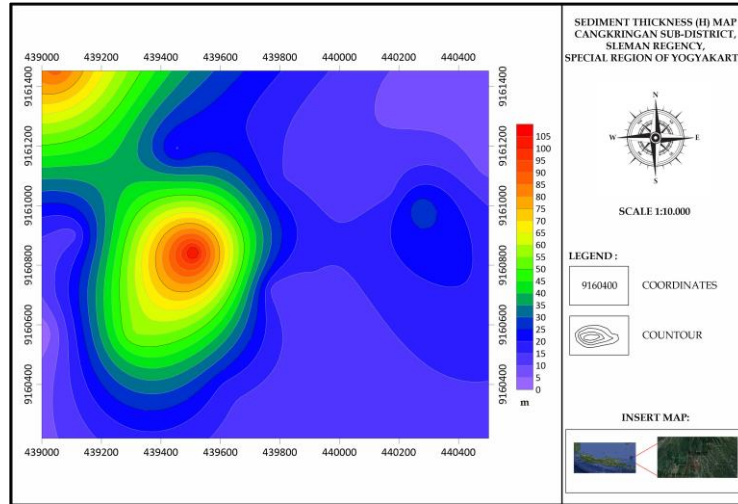


Figure 15. Map of Sediment Thickness (H) at the Research Location

Based on Figure 14, which is the map of sediment thickness distribution forming various color closures. Based on the color closures of the sediment thickness values above, it can be divided into three zones, namely shallow, moderate, and thick. The shallow sediment thickness zone is marked with blue, with thickness ranging from 0 to <30 meters. The moderate sediment thickness zone is marked with green to yellow with values ranging from >30 to <70 meters. Finally, the thick sediment thickness zone is marked with red, with values ranging from >70 to <105 meters. The variation in sediment thickness values relatively follows the same pattern as the geological characteristics of the study area, which is also based on the influence of topographic factors and variations in shear wave velocity (Satria, et al., 2020). Based on the sediment thickness map, the study area is dominated by blue closures, indicating that the study area has a shallow sediment layer. In the northwest part of the map, there is an area with a thick sediment layer indicated by the presence of red closures.

Determination of Mining Location Based on PGA, GSS, Soil Vulnerability, and Sediment Thickness Values

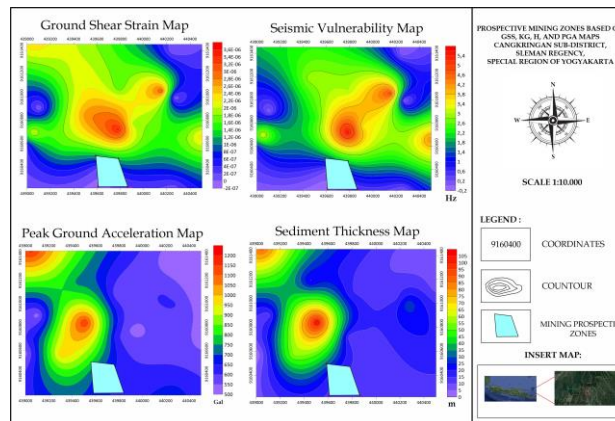


Figure 16. Map of GSS, Kg, PGA, and H in Determining Mining Prospects

The figure presents the analysis results of Ground Shear Strain (GSS), Seismic Vulnerability, Peak Ground Acceleration, and Sediment Thickness values. These

values are used to determine mining locations that fulfill environmental, disaster mitigation, and economic aspects based on sediment thickness. The GSS values indicate that the central area of the study has high values, represented by orange-red colors and values ranging from 2.4×10^{-6} to 3.6×10^{-6} . Moderate values are shown by green-yellow closures with values ranging from 1×10^{-6} to 2.2×10^{-6} , while low values are indicated by purple-blue closures with values from -2×10^{-7} to -8×10^{-7} . All these values are related to the same soil dynamic phenomenon, which is elastic wave and vibration. Regarding Soil Vulnerability (Kg), low values are considered appropriate, as lower values indicate less vulnerability to deformation. The low vulnerability, represented by purple-blue colors with values from -0.2 to 1.4, suggests subsurface conditions composed of hard rock/sediment with thin thickness. Additionally, for Peak Ground Acceleration (PGA), the study area falls within the range of 500-1200 gal. This is due to the area's association with Mount Merapi, which is classified as type A, often experiencing eruptions and soil movements. According to USGS, it falls under type X, indicating significant damage effects such as the collapse of walls, house frames, and foundations, damage to strong wooden structures, bridge collapses, and large landslides. Considering the sediment thickness obtained from microtremor data in the prospecting area, it is estimated to range from 0-35 m. Furthermore, based on 2.5 D gravity modeling on the north-south-oriented cross-section B-B', intersecting the study area, it shows that sediment thickness, as one moves away from Mount Merapi, increases. The estimated sediment thickness in that direction ranges from 20-90 meters from mean sea level (msl).

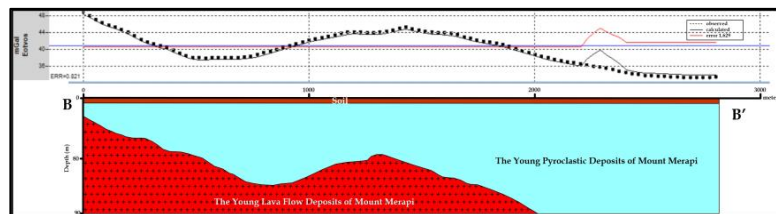


Figure 17. 2.5D Modeling Cross-Section 2 B-B' at the Research Location

Based on the analysis, the determination of the mining prospect zone is established at UTM coordinates -49 S with WGS84 datum in the research area in Cangkringan, Sleman, Yogyakarta. The prospective mining coordinates are at points 439588-9160495, 439783-9160472, 439610-9160232, 439864-9160231, situated along the Gendol Merapi River. These coordinates can contribute to restoring the Gendol River to its original condition, mitigating sediment buildup caused by the Merapi eruption. This aligns with the Sleman Regent Decree No. 284 of 2011 regarding the Normalization of River Flow Post-Merapi Eruption (Bahtiar, 2016; Putri & Raharjo, 2018; Nender, 2018; Anjani, 2021).

CONCLUSION

Based on the analysis conducted using parameters such as Peak Ground Acceleration and the Horizontal to Vertical Spectral Ratio (HVSr) outcomes, several findings have emerged in this discussion. It has been determined that the research area frequently experiences earthquakes or vibrations of intensity X, indicating significant and frequent seismic events. Moreover, the Ground Shear Strain data suggests potential seismic phenomena and exhibits elastic soil dynamics within the research area. Further

reinforcing this analysis is the soil vulnerability assessment, indicating that the area isn't prone to deformation but is susceptible to strong shaking due to the thickness of sediments and soft rocks. Additionally, the sediment thickness in the research area is estimated to range from 5-105 meters based on the secondary wave propagation velocity (V_s30). Furthermore, the research area is believed to consist of igneous rocks resulting from recent Merapi eruptions, estimated at depths of 40-100 meters with a density of 2.6 g/m³. The quantity of these rocks diminishes as the distance from Mount Merapi increases. Additionally, volcanic sediment layers, such as pyroclastic flows with a density of 2.1 g/m³, are estimated to have a thickness ranging from 0-100 meters. As one moves away from Mount Merapi, the quantity of sediment rocks is expected to increase. The research has also identified a potential mining prospect zone at UTM coordinates -49 S with a WGS84 datum in the study location, represented by specific coordinates: 439588-9160495, 439783-9160472, 439610-9160232, 439864-9160231.

REFERENCES

- Ainia, D. K., & Jirzanah. (2021). Analisis Deep Ecology Arne Naess terhadap Aktivitas Penambangan Pasir Merapi Studi Kasus: Penambangan Pasir Merapi di Sekitar Sungai Gendol Cangkringan Kabupaten Sleman. *Jurnal Ilmu Lingkungan*, 19(1), 98-106.
- Anjani, D. C. (2021). *Analisis Ketersediaan dan Kebutuhan Air Domestik di Desa Glagaharjo, Kecamatan Cangkringan, Kabupaten, Sleman, di Yogyakarta* (Doctoral dissertation, Universitas Gadjah Mada).
- Arifin, S. S. (2014). Penentuan Zona Rawan Guncangan Bencana Gempa Bumi Berdasarkan Analisis Nilai Amplifikasi HVSR Mikrotremor dan Analisis Periode Dominan Daerah Liwa dan Sekitarnya. *JGE (Jurnal Geofisika Eksplorasi)*, 2(01), 30-40.
- Bahtiar, A. (2016). Pelaksanaan Izin Usaha Pertambangan (IUP) Sebagai Upaya Pengendalian Kerusakan Lingkungan Akibat Penambangan Pasir di Kabupaten Sleman.
- Camus, G., Gourgaud, A., Mossand-Berthommier, P. C., & Vincent, P. M. (2000). Merapi (Central Java, Indonesia): an outline of the structural and magmatological evolution, with a special emphasis to the major pyroclastic events. *Journal of Volcanology and Geothermal Research*, 100(1-4), 139-163.
- Darmawan, H., Walter, T. R., Troll, V. R., & Budi-Santoso, A. (2018). Dome instability at Merapi volcano identified by drone photogrammetry and numerical modeling. *Nat. Hazards Earth Syst. Sci. Discuss*, 1-27.
- Directorate General of Water Resources (DGWR). (2010). *Study Report for Institution and Community Development. The Urgent Disaster Reduction Project for Mt. Merapi, Progo River Basin*. Ministry of Public Works, Indonesia.
- Fatimah, R. (2018). *Mikrozonasi Gempabumi Menggunakan Metode Mikroseismik di Desa Medana dan Jenggala Kecamatan Tanjung Kabupaten Lombok Utara* (Doctoral dissertation, Universitas Mataram).

- Gertisser, R., Charbonnier, S. J., Troll, V. R., Keller, J., Preece, K., Chadwick, J. P., ... & Herd, R. A. (2011). Merapi (Java, Indonesia): anatomy of a killer volcano. *Geology Today*, 27(2), 57-62.
- Gertisser, R., Charbonnier, S. J., Keller, J., & Quidelleur, X. (2012). The geological evolution of Merapi volcano, central Java, Indonesia. *Bulletin of Volcanology*, 74, 1213-1233.
- Gunawan, R., & Darmono. (2015). Studi Kasus Imbangan Angkutan Sedimen di Kali Putih. *Inersia: Jurnal Teknik Sipil dan Arsitektur*, 11(1), 90-94.
- Harsanto, P., Ikhsan, J., Pujianto, A., Hartono, E., Fitriadin, A. A., & Kuncoro, A. H. B. (2015). Karakteristik Bencana Sedimen Pada Sungai Vulkanik.
- Ishihara, K. (1982). Evaluation of Soil Properties for Use in Earthquake Response Analysis. *Proceedings International Symposium on Numerical Model in Geomech*, 237-259.
- Maimun, A. K., Silvia, U. N., & Ariyanto, P. (2020). Analisis Indeks Kerentanan Seismik, Periode Dominan, Dan Faktor Amplifikasi Menggunakan Metode Hvsr di Stageof Tangerang. *Jurnal Meteorologi Klimatologi dan Geofisika*, 7(2), 24-30.
- Nakamura, Y. (1989). A method for dynamic characteristics estimation of subsurface using microtremor on the ground surface. *Railway Technical Research Institute, Quarterly Reports*, 30(1).
- Nakamura, Y. (2000, January). Clear identification of fundamental idea of Nakamura's technique and its applications. In *Proceedings of the 12th world conference on earthquake engineering* (Vol. 2656, pp. 1-8).
- Nakamura, Y. (2008), *On The H/V Spectrum, The 14th World Conference on Earthquake Engineering October 12-17, 2008, Beijing, China*.
- Nender, A. C. (2018). Sinkronisasi Surat Keputusan Bupati Sleman Nomor 284/Kep. Kdh/A/2011 dengan Izin Usaha Pertambangan sebagai Usaha Pengendalian Kerusakan Lingkungan Akibat Penambangan Pasir di Kabupaten Sleman.
- Pancawati, K. D., Supriyadi, S., & Khumaedi, K. (2016). Identifikasi Kerentanan Dinding Bendungan dengan Menggunakan Metode Mikroseismik (Studi Kasus Bendungan Jatibarang, Semarang). *Unnes Physics Journal*, 5(2), 21-26.
- Putri, P. S., & Raharjo, T. (2018). Legal Mismatch on Illegal Sand Mining in Indonesia: an Example in Sleman, Indonesia. *Rechtsidee*, 4(2), 10-21070.
- PVMBG. (2014). *Gunung Merapi-Sejarah Letusan Laporan 03 June 2014*. Kementerian Energi dan Sumber Daya Mineral.
- Ratdomopurbo, A. (2008). Pedoman Mikrozonasi. *Materi Kursus*. Bandung: Tidak Dipublikasikan.
- Rahayu, R., Ariyanto, D. P., Komariah, K., Hartati, S., Syamsiyah, J., & Dewi, W. S. (2014). Dampak erupsi Gunung Merapi terhadap lahan dan upaya-upaya pemulihannya. *Caraka Tani: Journal of Sustainable Agriculture*, 29(1), 61-72.

- Saaduddin, S., & Marjiyono. (2015). Pemetaan Indeks Kerentanan Tanah Kota Padang Sumatera Barat dan Korelasinya dengan Titik Kerusakan Gempabumi 30 September 2009. Yogyakarta: Proceeding. In *Seminar Nasional Kebumihan ke-8*.
- Satria, A., Resta, I. L., & Nasri, M. Z. (2020). Analisis Ketebalan Lapisan Sedimen dan Indeks Kerentanan Seismik Kota Jambi Bagian Timur. *JGE (Jurnal Geofisika Eksplorasi)*, 6(1), 18-30.
- Sungkono, B. J. (2011). Karakterisasi Kurva Horizontal-To-Vertical Spectral Ratio: Kajian Literatur Dan Permodelan. *Jurnal Neutrino: Jurnal Fisika dan Aplikasinya*, 4(1), 1-15.
- Swastika, P. (2020). *Analisis Variasi Dasar Sungai Gendol Pada Hulu Sabo Dam GE-D5 Dengan Teknik Fotogrametri* (Doctoral dissertation, Universitas Gadjah Mada).
- Syahputri, A., & Sismanto, S. (2020). Identifikasi Potensi Tanah Longsor Menggunakan Metode Mikrotremor Di Dusun Tegalsari Desa Ngargosari Kecamatan Samigaluh Kabupaten Kulon Progo. *Jurnal Fisika Indonesia*, 24(2), 66-71.
- USGS. (2016). *Search Earthquake Catalog*. Diakses dari: <https://earthquake.usgs.gov/>
- Uwiduhaye, J., Mizunaga, H., & Saibi, H. (2016). 2-D Forward Modelling of Gravity Data, A Case Study of Kinigi Geothermal Field, Rwanda. In *Proceedings of the 135th SEGJ Conference* 135.
- Wibowo, N. B., & Huda, I. (2020). Analisis Amplifikasi, Indeks Kerentanan Seismik Dan Klasifikasi Tanah Berdasarkan Distribusi Vs30 DI Yogyakarta. *Buletin Meteorologi, Klimatologi, Dan Geofisika*, 1(2), 21-31.
- Wirakusumah, A., Juwarna, H., & Loebis, H. (1989). *Peta Gunungapi Merapi, Provinsi Daerah Istimewa Yogyakarta & Jawa Tengah*. Bandung: Badan Geologi.
- Yudiantoro, D. F., & Paramita Haty, I. (2023). Analisis Deformasi Gunung Api Merapi, Melalui Penerapan Metode Kombinasi Block Movement dan Deformasi Elastis, Pada Periode Tahun 1995-1997 Berdasarkan Data Gps (Global Positioning System). *Jurnal Ilmiah Geologi Pangea*, 10, 45-60.
- Zuidam, R. V. (1983). *Guide to Geomorphic Aerial Photographic Interpretation and Mapping*, ITC.